Fundamental Research 3 (2023) 37–44

Contents lists available at ScienceDirect

Fundamental Research

journal homepage: http://www.keaipublishing.com/en/journals/fundamental-research/

Article

Phonon and photon lasing dynamics in optomechanical cavities

Jian Xiong[a,b,1], Zhilei Huang[a,b,1], Kaiyu Cui[a,b,*], Xue Feng[a,b], Fang Liu[a,b], Wei Zhang[a,b,c], Yidong Huang[a,b,c,*]

[a] Department of Electronic Engineering, Tsinghua University, Beijing 100084, China
[b] Beijing National Research Center for Information Science and Technology, Beijing 100084, China
[c] Beijing Academy of Quantum Information Science, Beijing 100193, China

ARTICLE INFO

Article history:
Received 8 July 2022
Received in revised form 12 September 2022
Accepted 5 October 2022
Available online 25 October 2022

Keywords:
Nonlinear optics
Optomechanical Crystal
Cavity optomechanics
Phonon lasing
Limit cycle

ABSTRACT

Lasers differ from other light sources in that they are coherent, and their coherence makes them indispensable to both fundamental research and practical application. In optomechanical cavities, photon and phonon lasing is facilitated by the ability of photons and phonons to interact intensively and excite one another coherently. The lasing linewidths of both phonons and photons are critical for practical application. This study investigates the lasing linewidths of photons and phonons from the underlying dynamics in an optomechanical cavity. We find that the linewidths can be accounted for by two distinct physical mechanisms in two regimes, namely the normal regime and the reversed regime, where the intrinsic optical decay rate is either larger or smaller than the intrinsic mechanical decay rate. In the normal regime, an ultra-narrow spectral linewidth of 5.4 kHz for phonon lasing at 6.22 GHz can be achieved regardless of the linewidth of the pump light, while these results are counterintuitively unattainable for photon lasing in the reversed regime. These results pave the way towards harnessing the coherence of both photons and phonons in silicon photonic devices and reshaping their spectra, potentially opening up new technologies in sensing, metrology, spectroscopy, and signal processing, as well as in applications requiring sources that offer an ultra-high degree of coherence.

1. Introduction

As the strongest and most tunable nonlinear interaction, the photon-phonon interaction can be harnessed in both classical and quantum regimes [1]. Brillouin scattering, which results from interactions between photons and travelling acoustic phonons, has shown considerable potential for high-coherence and ultra-low-noise oscillation owing to the unique lasing dynamics of stimulated Brillouin scattering (SBS) [2–4]. SBS in ordinary optical materials such as glass has facilitated a range of technological applications in metrology [5], sensing [6,7], and signal processing [8,9]. However, achieving SBS in silicon, the fundamental material underlying photonic integrated circuits, is challenging because the acoustic wave in a silicon waveguide irreversibly radiates into the silica cladding layer. Specifically, Brillouin lasing [10] and modulation [11] are possible only through the use of silicon waveguides that are several centimetres long and suspended in air [12,13]. It is technically challenging to build such structures, which are important for laser technologies based on silicon [10–13].

Photon-phonon interactions can be greatly enhanced by optomechanical cavities [14,15]. Such cavities have facilitated the demonstration of many significant phenomena [16–19]. For example, phonon lasers, which are mechanical analogues of photon lasers, have attracted considerable attention owing to their underlying intriguing physics [20–23] and unprecedented capability for ultra-precise sensing [24,25]. The linewidth limit of phonon lasers is theoretically predicted to follow a Schawlow–Townes form, similar to that of photon lasers [26]. In addition, the optomechanical limit cycle theory [27] has been developed as an efficient tool for studying the physics of lasing dynamics, providing analytical solutions of the phonon linewidth with thermal noise in the normal regime [28]. For cavity optomechanical systems, this theory has successfully explained the dynamical multistability phenomenon [29], amplitude noise suppression [30], and phase noise using linear approximation of the Langevin equation [28]. Despite these significant theoretical advances, the phase noise of the pump light, which severely limits the realisation of ultra-narrow linewidth for photon and phonon lasers in practice, has not been considered in theoretical studies thus far.

Phase noise, which varies inversely with oscillator energy in accordance with the classical theory, has been experimentally observed with phonon lasers [31,32]. Other experimental studies have shown that, after phonon lasing, the photons scattered by phonons exhibit coherent light conversion [33]. Such coherent conversion is not only important in the quantum regime [16] but also indicates that optomechan-

* Corresponding authors.
E-mail addresses: kaiyucui@tsinghua.edu.cn (K. Cui), yidonghuang@tsinghua.edu.cn (Y. Huang).
[1] These authors contributed equally to this work.

https://doi.org/10.1016/j.fmre.2022.10.008
2667-3258/© 2022 The Authors. Publishing Services by Elsevier B.V. on behalf of KeAi Communications Co. Ltd. This is an open access article under the CC BY-NC-ND license (http://creativecommons.org/licenses/by-nc-nd/4.0/)

ical cavities may offer a solution for reshaping the spectra and coherence of both photons and phonons, which can be used in the fields that require highly coherent sources. Coherent photon-phonon interactions may also complement silicon-based Brillouin lasers [10,34]. The optical self-oscillation and true line narrowing to the Schawlow–Townes limit have been reported to require the reversed dissipation regime in Brillouin lasers [35]. However, in contrast to a previous study [36], we find that high-coherence and ultra-low-noise oscillation for the scattered light in optomechanical cavities is counter-intuitively unattainable in the reversed regime, which is because linearized optomechanical equations are used in the previous study (Supplementary S1-S2) and this approach expires in the reversed regime. Since the linewidth features of photon and phonon are critical to a wide range of practical applications, it is necessary to reanalyse the lasing dynamics with phase noise and take nonlinear nature of the optomechanical system into consideration.

This study revealed the lasing linewidths of photons and phonons in a cavity optomechanical system. The lasing dynamics considering both the pump noise and the thermal noise are explored by a general limit cycle theory without linearisation approximation. For simplicity, the lasing phenomena are explained in both normal and reversed regimes. The general expressions of the analytical solutions for the lasing linewidth are obtained, which are in good agreement with the numerical analysis. The linewidth-narrowing mechanism can be explained on the basis of a phase-noise-following scenario, and the ultra-narrow spectral linewidth for phonon lasing can be realised regardless of the linewidth of the pump light. However, such results are counterintuitively unattainable for photon lasing, which differs significantly from a Brillouin system. In a silicon-based optomechanical crystal (OMC) cavity, we experimentally observe phonon lasing of frequency up to 6.22 GHz, with the scattering photon stimulated at a communication-relevant wavelength of 1533.9 nm. The optomechanical coupling rate of the cavity is 1.9 MHz. The observed linewidth of the excited phonon decreases to 5.4 kHz, which is four orders of magnitude narrower than the linewidth of the pump light, whereas the linewidths of the scattering photon and pump light are similar, which is in agreement with our theoretical predictions.

2. Methods

2.1. Simulation of the lasing dynamics

The differential evolution equations of the optomechanical systems were solved numerically using the Runge–Kutta method. The time step was set to 0.01 of the mechanical period. To emulate the Gaussian noise due to the thermal force as well as the phase noise of the pump light, Gaussian-distributed stochastic quantities were introduced that were invariant in the same step and changed between different steps. To obtain the power spectra in the frequency domain, the optical amplitude and displacement in the time domain were Fourier-transformed, and the square norms were applied.

2.2. Fabrication of the lasing cavity

The patterns of the cavities were first defined by electron beam lithography and then transferred to a silicon-on-insulator (SOI) wafer with a device layer of 220 nm by inductively coupled plasma etching. Subsequently, the buried oxide layers beneath the cavities were removed by wet etching with buffered hydrofluoric acid to form the suspended structures.

2.3. Measurements

A tunable laser light source was used. The cavities were optically coupled using a tapered fiber, and the output was split into two channels. One port was connected to a low-frequency (kHz) optical power monitor, from which the optical spectrum was obtained by sweeping the wavelength of the laser. The other port was connected to a high-frequency (12.5 GHz) optical receiver, and its output was connected to an electrical spectrum analyser to obtain the mechanical spectra (Supplementary S10).

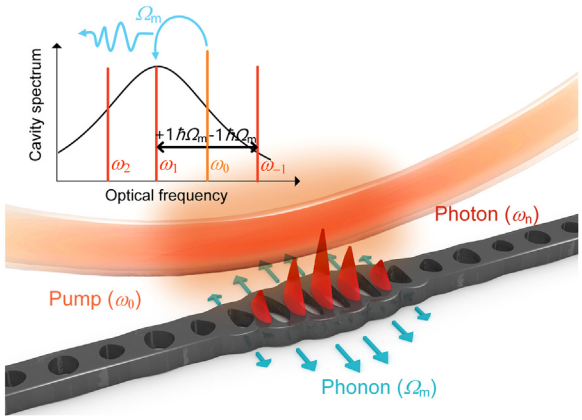

Fig. 1. Schematic of photon/phonon lasing. The pump photons (shown in orange, ω_0), which are coupled to the cavity with a tapered fiber, are transferred to the scattering photons (shown in red, including the high-order scattering light), and they excite the phonons (shown in blue). The photon with frequency ω_n represents the scattering photon converted from the pump photon by releasing n phonons.

To conduct the lasing experiment, we blue-detuned the tunable laser, i.e. we set the wavelength of the laser below the cavity wavelength. To eliminate the effect of the optical frequency shift of the cavity owing to thermal noise, the wavelength of the tunable laser was tuned to deliver the highest power in the electrical spectrum analyser for each input power, ensuring a fixed detuning between the pump and the cavity (Supplementary S7). For example, because the ratio between the mechanical frequency and the total optical decay rate (Ω_m/κ) was 0.21 for the OMC cavity, the largest signal from the electrical spectrum analyser was obtained when the ratio between the optical detuning and the total optical decay rate (Δ/κ) was 0.31.

3. Results

3.1. Lasing dynamics of phonons and scattering photons

In a cavity optomechanical system, the light interacts with the mechanical motion, which affects the effective mechanical damping rate. When we blue-detune the pump light and increase its power, the effective mechanical damping can be not only reduced to zero but also changed to amplification. Accordingly, coherently self-sustained oscillation, i.e. phonon lasing, and stimulated photon scattering can occur with coherent light conversion. The combination of phonon lasing and stimulated photon scattering is shown in Fig. 1. The experimental data in this figure indicate that large energy accumulation of phonons and photons will occur simultaneously if the pump power exceeds the laser threshold (Supplementary S1).

For the cavity optomechanical system, the interaction Hamiltonian between a photon and a phonon can be written as $-\hbar g_0 \hat{a}^\dagger \hat{a}(\hat{b}^\dagger + \hat{b})$, where $\hbar$ is the reduced Planck constant, g_0 is the vacuum optomechanical coupling strength, and $\hat{a}(\hat{a}^\dagger)$ and $\hat{b}(\hat{b}^\dagger)$ are the annihilation (creation) operators of photons and phonons, respectively [37]. Based on this interaction Hamiltonian, the evolution equations of the cavity system can be derived in the semi-classical regime as

$$\dot{a} = (i\Delta - \kappa/2)a + ig_0(b^* + b)a + \sqrt{\kappa_{ex}}s_{in} \tag{1}$$

$$\dot{b} = -(i\Omega_m + \Gamma/2)b + ig_0|a|^2 + \sqrt{\Gamma}b_{th} \tag{2}$$

where a is the optical amplitude in the cavity; Δ represents the laser detuning from the cavity resonance, i.e. ω_0-ω_1, where ω_1 is the optical angular frequency of the cavity and ω_0 is the angular frequency with which the frame rotates with the pump laser; κ is the total decay rate of the optical mode; κ_{ex} is the optical coupling rate between the optical input channel and the cavity; b is the mechanical amplitude that satisfies $x = x_{zpf}(b + b^*)$, where x is the displacement of the mechanical cavity and x_{zpf} denotes the zero-point fluctuation displacement; Ω_m represents the intrinsic angular frequency of the mechanical mode; Γ is the decay rate of the mechanical mode; b_{th} is the noise of the mechanical oscillator owing to the thermal fluctuations in the environment, which is expressed as $b_{th} = \sqrt{n_{th}}\dot{W} = \sqrt{k_B T/\hbar\Omega_m}\dot{W}$, where n_{th} is the number of phonons in the thermal equilibrium state k_B is the Boltzmann constant, T denotes temperature, and W is the standard Wiener process [38]; and s_{in} is the amplitude of the pump light [39,40]. As the intensity noise can be ignored for a typical single-mode laser, the linewidth of the pump laser originates from the phase noise [34,41]. Thus$s_{in} = |s_{in}|e^{i\varepsilon_p}$, where $\varepsilon_p = \sqrt{v_p}W$ and $v_p = \mathrm{var}(\dot{\varepsilon}_p)$ is the angular frequency linewidth of the pump laser [42].

According to the limit cycle theory, the scattering photons and phonons in the cavity can be written in the form of a Fourier series expansion, i.e. $b = B_c + Be^{-i\Omega_m t}$ and $a = \sum_n \alpha_n e^{in\cdot\Omega_m t}$, where B_c represents the equilibrium position of the mechanical vibration and B is the normalised complex amplitude of the mechanical vibration (including the amplitude B_0 and the phase ϕ, i.e. $b = B_c + B_0 e^{i\phi}e^{-i\Omega_m t}$). Here, we consider that the mechanical vibration mode with multiple frequencies of Ω_m usually has a large dissipation rate such that only the first harmonic term is retained [28]. Further, α_n is the normalised complex amplitude of photons with different frequencies ω_n in the cavity, i.e. $\alpha_n = A_n e^{i\varepsilon_n}$ (A_n is the amplitude of the optical field and ε_n is the corresponding phase). The subscript n implies that the scattering photon with index n comes from the pump photon after releasing n phonons. For instance, α_0 ($A_0 e^{i\varepsilon_0}$) represents the normalised complex amplitude of the photon with frequency ω_0. By applying Fourier series expansion of a and b to Eqs. 1 and 2, the equations for analysing the phase dynamics can be obtained (Supplementary S3).

$$\dot{\phi} = \frac{M\Gamma}{2}\cos(\phi + \varepsilon_1 - \varepsilon_0) + \frac{\sqrt{\Gamma}}{\langle B_0\rangle} b_{th}\sin(\Omega_m t - \phi) \tag{3}$$

$$\dot{\varepsilon}_1 = \tilde{\Delta} - \Omega_m + \frac{M\kappa}{2}\cos(\phi + \varepsilon_1 - \varepsilon_0) \tag{4}$$

$$\dot{\varepsilon}_0 = \tilde{\Delta} + g_0\left\langle\frac{B_0 A_1}{A_0}\right\rangle\cos(\phi + \varepsilon_1 - \varepsilon_0) + \frac{\sqrt{\kappa_{ex}}|s_{in}|}{\langle A_0\rangle}\sin(\varepsilon_p - \varepsilon_0) \tag{5}$$

The above-mentioned equations are the phase reduction equations, which are often used to analyse the phase evolution and synchronisation phenomena in the self-sustained oscillating system [43]. Here, M is a nonlinear factor that characterises the strength of the pump and $\tilde{\Delta}$ represents the equivalent detuning. When the system is lasing, the phonon phase ϕ, the scattering photon phase ε_1, and the pump light phase ε_p need to be synchronised (Supplementary S3–2). In this paper, we introduce this phase synchronisation condition to solve Eqs. 3–5. Based on the phase reduction equations, the angular frequency linewidths of the phonon (v_m) and the scattering photon (v_s) can be obtained from the variance of the derivative of phase:$v_m = \mathrm{var}(\dot{\phi})$ and $v_s = \mathrm{var}(\dot{\varepsilon}_1)$. We need to consider only the random variables, namely ϕ, ε_0, ε_1, b_{th}, and $\tilde{\Delta}$ on the right-hand side of Eqs. 3–5, as the constant terms do not affect the linewidth. First, we analyse the influence of $\tilde{\Delta}$. The fluctuation strength of $\tilde{\Delta}$ can be derived as follows (Supplementary S3–1):

$$\tilde{\Delta} = \Delta + 2g_0\mathrm{Re}[B_c] = \Delta + \chi^{(2)}\sum|a_n|^2 \tag{6}$$

$$\begin{aligned}\delta\tilde{\Delta} &= \tilde{\Delta} - \langle\tilde{\Delta}\rangle = 2\chi^{(2)}\sum A_n\delta A_n \cdot (\textit{keep the first}-\textit{order fluctuation term})\\ &= 2\chi^{(2)}(A_1\delta A_1 + A_0\delta A_0)\cdot(\textit{use the sideband resolved assumption})\\ &= 2\chi^{(2)}[(\Gamma/\kappa)B_0\delta B_0 + A_0\delta A_0]\\ &\quad\cdot(\textit{use the energy conservation relation } A_1/B_0 = \sqrt{\Gamma/\kappa})\end{aligned} \tag{7}$$

It can be concluded from Eq. 6 that $\tilde{\Delta}$ comes from the random jitter of the equilibrium position B_c, which is determined by the radiation pressure. Hence, $\tilde{\Delta}$ is associated with the intra-cavity field strength $\sum|a_n|^2$ and is thus affected by the fluctuation of the intra-cavity field intensity. From the expression of $\tilde{\Delta}$, $\delta\tilde{\Delta}$ can be derived as Eq. 7. Here, $\chi^{(2)} = 2g_0^2/\Omega_m$ is the equivalent Kerr nonlinear coefficient [27], which indicates the influence of the field intensity on the effective cavity length. Further, $\delta A_n = A_n - \langle A_n\rangle$ represents the amplitude noise of the nth-order scattering photon. When there are fluctuations in the field intensity, the equivalent cavity length will undergo random jitter. As the amplitude noise in the limit cycle oscillator is suppressed [30], only the first-order fluctuation term needs to be retained.

It can be seen that the effective detuning $\delta\tilde{\Delta}$ is directly associated with the dissipation rate Γ/κ. For the normal regime ($\Gamma \ll \kappa$), the ratio of Γ/κ is considerably small; hence, we can ignore the first term. Moreover, the pump strength A_0 can also be ignored because a phonon with a sufficiently low dissipation rate requires only a low-power pump to achieve lasing. Note that in this regime, treating $\tilde{\Delta}$ as a constant is a common strategy [37]. Through the analysis presented above, we conclude that $\delta\tilde{\Delta}$ can be ignored in the normal regime. However, the situation is different for the reversed regime. In this case, we can still ignore A_0 because there is only one dominant optical mode ω_1 in this regime [36] (see Supplementary Information Fig. S2 for details). However, the first term in Eq. 7 cannot be ignored owing to the large ratio of Γ/κ. Hence, the fluctuation in the effective detuning $\delta\tilde{\Delta}$ will be remarkable in the reversed regime. As the effects of $\delta\tilde{\Delta}$ on the linewidth characteristics are different in the two regimes, we will discuss these two regimes separately. In addition, we will directly solve the temporal stochastic differential equation for Eqs. 1 and 2 numerically without any approximation to validate our theoretical results.

Normal regime ($\Gamma \ll \kappa$): As the mechanical decay rate is much smaller than the optical decay rate, the phonons can be accumulated more effectively compared with the photons. Thus, $\tilde{\Delta}$ can be treated as a constant, i.e. $\tilde{\Delta} \approx \Delta$, which can be derived from Eq. 6 as well when the jitter of the intra-cavity light field strength $\sum|a_n|^2$ is negligible. Under this condition, we obtain the linewidths of both the scattering photons and the phonons by solving the phase reduction Eqs. 3–5 (Supplementary S3–3-1):

$$v_s = v_{mT} + \frac{v_p}{(1+\Gamma/\kappa)^2} \tag{8}$$

$$v_m = v_{mT} + \frac{v_p}{(1+\kappa/\Gamma)^2} \tag{9}$$

$$v_{mT} = \frac{\Gamma n_{th}}{2n} \tag{10}$$

The linewidth expression above is divided into two parts. One part is the linewidth of the Schawlow–Townes (ST) type, v_{mT}, which is inversely proportional to the number of intra-cavity phonons n. When the ratio of n to the number of thermal equilibrium phonons n_{th} is large, the broadening of the linewidth owing to thermal noise will be strongly suppressed. The ST linewidth formula derived from our equations is consistent with that obtained by Kerry J. Vahala [26]. The other part is the linewidth broadening owing to the phase noise of the non-ideal pumping light source, which is similar to the linewidth in SBS [34]. Besides the analytical expressions for the lasing linewidth, in the normal regime ($\Gamma \ll \kappa$), we can also obtain the important relation $\dot{\varepsilon}_1 = \tilde{\Delta} - \Omega_m + (\kappa/\Gamma)\dot{\phi}$ (derived from Eqs. 3 and 4 by ignoring the thermal noise). Further, by assuming that $\tilde{\Delta} \approx \Omega_m$, the simplified expression $\dot{\varepsilon}_1 = (\kappa/\Gamma)\dot{\phi}$ can be

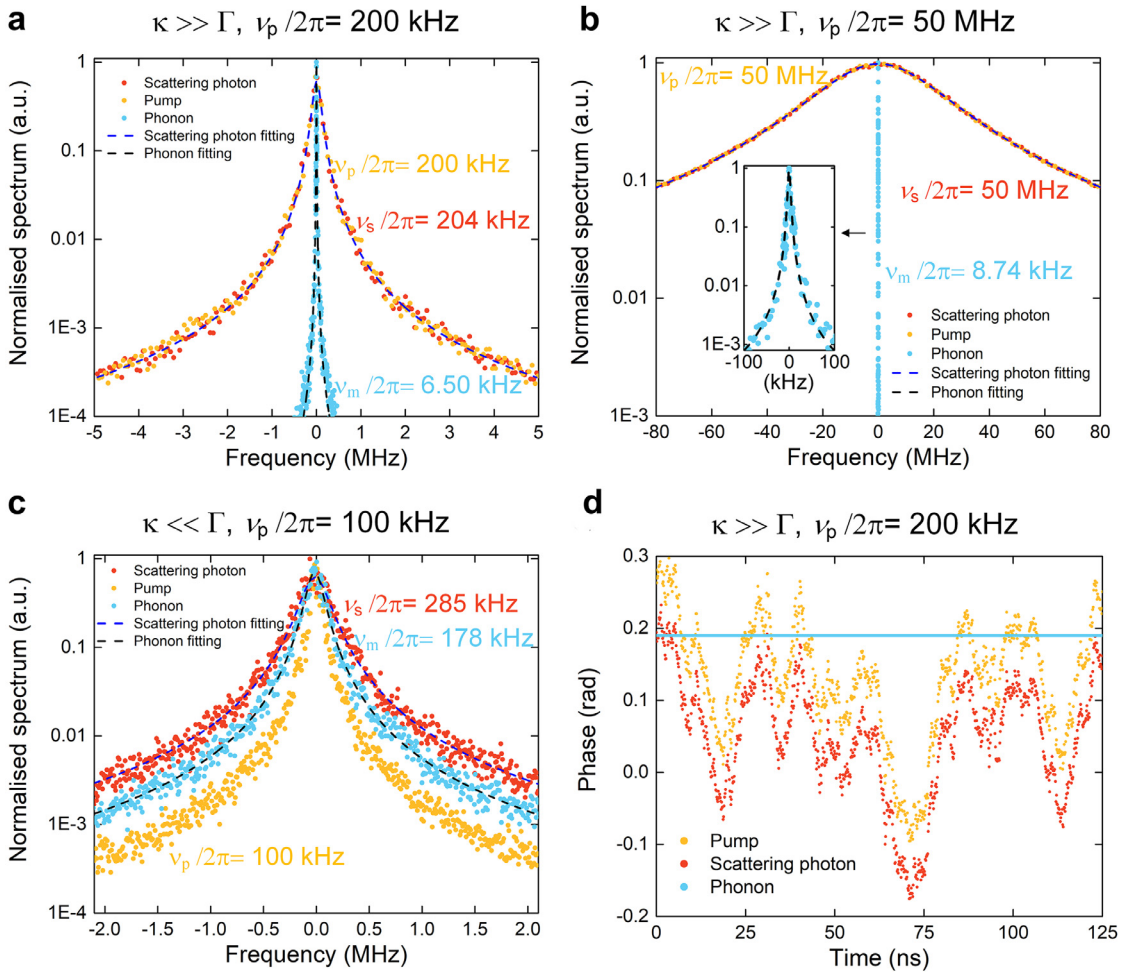

Fig. 2. Simulated photon and phonon lasing results. (a)–(c) Spectra of the pump, scattering photon, and phonon (mechanical motion) after lasing. The linewidth values marked in the figure are obtained from the Lorentz fitting. Further, we use the derived analysis expressions (8), (9), and (13) to calculate the theoretical linewidths. They are consistent with the Lorentz fitting. Results obtained with a cavity in the normal regime ($\Gamma \ll \kappa$) at a pump-laser linewidth of (a) 200 kHz and (b) 50 MHz. (c) Results of the cavity in the reversed regime ($\Gamma \gg \kappa$) with a pump-laser linewidth of 100 kHz. (d) Phase fluctuation of the pump, scattering photon, and phonon after lasing in the normal regime ($\Gamma \ll \kappa$) with a pump-laser linewidth of 200 kHz for the system represented in a.

obtained. This is a good theoretical support for the approximation of $\dot{\phi} \ll \dot{\varepsilon}_1$, which is widely used in the normal regime without detailed theoretical explanation [27,30,44].

We also directly solve the temporal stochastic differential equation for Eqs. 1 and 2 numerically, and we use Fourier transform to obtain the spectrum in the frequency domain. The spectra are shown in Fig. 2.

For the normal regime, Fig. 2a shows the simulated spectrum of the cavity optomechanical system after lasing. The parameters were set as $\kappa/2\pi = 30\text{GHz}$, $\Omega_m/2\pi = 6.2\text{GHz}$, and $\Gamma/2\pi = 3.2\text{MHz}$, which were the values in our experiments. The linewidth of the pump light ($\nu_p/2\pi$) was set to $2.0 \times 10^2\text{kHz}$. We can see that after lasing, the spectral linewidth of the scattering photon ($\nu_s/2\pi$) is around $2.0 \times 10^2\text{kHz}$, which is nearly the same as that of the pump light. By contrast, the spectral linewidth of the phonon ($\nu_m/2\pi$), which is around 6.5 kHz, is much narrower than that of the pump light. The spectral linewidths are also calculated on the basis of the analytical expressions of Eqs. 8 and 9. The calculated $\nu_s/2\pi$ and $\nu_m/2\pi$ are about 206.35 kHz and 6.35 kHz, respectively, which are in good agreement with the numerical analysis.

These results indicate that the phonon linewidth is several orders of magnitude narrower than that of the scattering photon for a cavity with $\Gamma \ll \kappa$ after lasing. To further understand the reason for this difference, the phase noise of the scattering photon and phonon was simulated (Fig. 2d). We find that the scattering photon follows the phase fluctuations of the pump light, while the phonon preserves its phase because the damping rate of the scattering photon is greater than that of the phonon. We can also use the adiabatic approximation to understand the transmission mechanism of the phase noise of the pump light. When the phonon dissipation rate is extremely low, the phonon is nearly adiabatic, which means that it needs nearly no assistance from the pump to maintain its stability. Hence, the phase noise of the pump light cannot be transmitted to the phonon, and the broadening of the phonon spectral line can thus be ignored, which is also indicated by the narrowing factor $(1 + \kappa/\Gamma)^2 \to \infty$ in Eq. 9. However, the scattering photon has a large dissipation rate and thus succeeds the phase fluctuations of the pump light, which is shown by the narrowing factor $(1 + \Gamma/\kappa)^2 \to 1$ in Eq. 8. When the optomechanical cavity is at room temperature, for the normal regime ($\Gamma \ll \kappa$), the thermal noise dominates the linewidth of the phonon with an ST-type formula [26].

Note that phonon lasing can also be excited by a pump whose linewidth is much greater than the intrinsic mechanical linewidth. For instance, the parameter setting for the simulation shown in Fig. 2b is the same as that shown in Fig. 2a, except that $\nu_p/2\pi$ was changed to 50 MHz, which was much greater than the intrinsic mechanical linewidth of 3.3 MHz. As can be seen in Fig. 2b, mechanical oscillation can also be excited by this high-noise pump light with a linewidth of 8.74 kHz, because the ST linewidth is dominant in this regime and the change in the pump linewidth thus has a very small impact on the phonon. The slight broadening of the phonon linewidth is owing to the decrease of

the phonon number, which is caused by the increased linewidth of the pump. This ultra-narrow linewidth has considerable potential for applications in various fields such as high-precision sensing, high-quality frequency references, frequency-coherent conversion [45], and low-noise phonon sources [46].

Reversed regime($\Gamma \gg \kappa$): This spectral region is beyond the scope of existing silicon-based microstructures because the required optical Q-factor is rather high (typically, it needs to exceed 3.2×10^8 for a 6-GHz mechanical mode with a Q-factor of 1×10^3 and $\Gamma/\kappa = 10$). However, this scenario can be realised in the microwave domain [47]. Nevertheless, an important question is whether the scattering photon undergoes linewidth narrowing similar to the phenomenon in the case of a Brillouin laser regardless of the materials used or the design of the structures employed.

To answer this question, we must re-examine the linewidth of the scattering photon and phonon from Eqs. 3 to 5 by considering the influence of the equilibrium position. (a) The driving force (radiation pressure) term of the mechanical vibration is the beat note of the scattering light and pump light, which is related only to their relative phase difference $\varepsilon_1 - \varepsilon_0$. (b) The modulation due to the jitter in the equilibrium position is the same for every intra-cavity optical spectrum line. Therefore, the random phase of the phonon, which is determined only by the beat note of the optical line, will not be affected by such jitter and it still satisfies Eq. 9, which means that in the reversed regime ($\Gamma \gg \kappa$), $\nu_m \approx \nu_p/(1+\kappa/\Gamma)^2 + \nu_{mT}$. This conclusion can also be drawn from the interaction picture, i.e. the jitter in the equilibrium position can modulate the phase of the photons by the scattering process, but there is no direct interaction between the mechanical vibration and the cavity length. Hence, the phase of the phonons should not be affected. To further analyse the linewidth of the scattering photons, we define $\dot{\varepsilon}_c = \delta\tilde{\Delta}$ representing the random phase diffusion due to the jitter of the equilibrium position such that the original phase of the photons before perturbation by the jitter can be separated, i.e. $\dot{\varepsilon}'_n = \dot{\varepsilon}_n - \dot{\varepsilon}_c$. In this manner, Eqs. 4 and 5 can be reduced to (Supplementary S3–3-2)

$$\dot{\varepsilon}'_1 = \left\langle \tilde{\Delta} \right\rangle - \Omega_m + \frac{M\kappa}{2} \cos\left(\phi + \varepsilon_1 - \varepsilon_0\right) \tag{11}$$

$$\dot{\varepsilon}'_0 = \left\langle \tilde{\Delta} \right\rangle + g_0 \left\langle \frac{B_0 A_1}{A_0} \right\rangle \cos\left(\phi + \varepsilon_1 - \varepsilon_0\right) + \frac{\sqrt{\kappa_{ex}}\left|s_{in}\right|}{\langle A_0 \rangle} \sin\left[(\varepsilon_p - \varepsilon_c) - \varepsilon_0\right] \tag{12}$$

If $(\varepsilon_p - \varepsilon_c)$ is considered to be the pseudo pump phase, when we ignore $\delta\tilde{\Delta}$ in Eqs. 3–5, the form of Eqs. 3, 11, and 12 is similar to that of Eqs. 3–5. Thus, we can use the same method as that for the normal regime to obtain the linewidth formula. Combining the relation $\nu_m \approx \nu_{mT} + \nu_p/(1+\kappa/\Gamma)^2$ derived above, we obtain (Supplementary S3–3-2)

$$\nu_s = \nu_{mT} + 2\nu_p + \nu_p/(1+\Gamma/\kappa)^2 \approx \nu_{mT} + 2\nu_p \tag{13}$$

$$\nu_m = \nu_{mT} + \frac{\nu_p}{(1+\kappa/\Gamma)^2} \cdot (\textit{phonon linewidth formula is the same in both regimes})$$

$$\nu_{mT} = \frac{\Gamma n_{th}}{2n} \cdot (\textit{ST linewidth formula is the same in both regimes})$$

In the reversed regime ($\Gamma \gg \kappa$), owing to the strong jitter in the equilibrium position, the phase noise of the pump can be transmitted to the scattering photons, which overcomes the adiabatic approximation of the scattering photons. Thus, even if the intensity of the intra-cavity scattering photons is high when the system is lasing, the scattering photon linewidth ν_s cannot reach the ST limit, which implies that the self-purifying spectral line of the scattering photons, similar to that exhibited in SBS of the photon laser regime, is impossible to achieve in optomechanical cavities. Further, if we accidentally ignore the jitter in the equilibrium position (high-order terms of the interaction Hamiltonian), we can, by contrast, conclude that the spectral line can be narrowed to the ST limit [36]. This discrepancy is counterintuitive when compared with the Brillouin system, because there is no equilibrium position for the travelling acoustic wave in the Brillouin system.

The numerically simulated spectrum after lasing for a cavity optomechanical system with $\Gamma \gg \kappa$ in the reversed regime is shown in Fig. 2c. Here, we set $\kappa/2\pi = 6.5$ MHz, $\Gamma/2\pi = 197$ MHz, and $\nu_p/2\pi = 100$kHz in the simulation. As shown in Fig. 2c, $\nu_s/2\pi$ and $\nu_m/2\pi$, with simulated values of about 285 kHz and 178 kHz, respectively, are both broader than the linewidth of the pump light. From Eqs. 9 to 13, the calculated linewidths $\nu_s/2\pi$ and $\nu_m/2\pi$ are 285.8 kHz and 185.8 kHz ($\nu_{mT}/2\pi = 85.8$kHz), which indicates that the theoretical analysis is well consistent with our simulation results.

To summarise the lasing dynamics, we find that the linewidth of photon and phonon lasing can be explained and analysed with reference to two distinct physical regimes ($\Gamma \ll \kappa$ and $\Gamma \gg \kappa$). For the normal regime ($\Gamma \ll \kappa$), the linewidth of the phonon is much narrower than that of the pump laser, and the ultra-low-noise mechanical signal can be excited even with a high-noise pump light whereas the linewidths of the scattering photon and pump light are similar. This linewidth-narrowing mechanism is similar to that of the Brillouin laser, except that the roles of the phonon and the scattering photon are reversed, as the typical Brillouin system satisfies the $\Gamma \gg \kappa$ condition. Meanwhile, for the reversed regime ($\Gamma \gg \kappa$), the linewidths of both the scattering photon and the phonon are broader than the linewidth of the pump light. The counterintuitive linewidth of the scattering photon originates from the jitter in the equilibrium position of the optomechanical cavity system and it differs significantly from that of the Brillouin system.

3.2. OMC cavity with acoustic radiation shield

An OMC cavity with an acoustic radiation shield was fabricated to demonstrate the photon and phonon lasers in practice. An oblique view of a scanning electron microscope (SEM) image of the structure is shown in Fig. 3a. The confinement mechanism of this structure is different from that of conventional OMC cavities, where the optical and mechanical modes are simultaneously confined by the same periodic structure [48]. As the mechanical frequency of this structure exceeds the phononic bandgap of nanobeam periodic structures, the nanobeam periodic structures of this OMC cavity can only confine the optical mode. By contrast, the acoustic radiation shield shown in Fig. 3b confines the mechanical mode as its phononic bandgap covers the mechanical frequency (Supplementary S4). Thus, the optical and mechanical modes are separately confined by two types of structures. This confinement mechanism is used to overcome the design constraints of the optical and mechanical properties [49]. This flexible design by separate confinement mechanism can be used in many research areas, for instance, intrinsic defect induced Eps [50–52] and phonon sensing [25], etc. Benefit from the flexible design, the mechanical frequency of the cavity reaches 6.22 GHz while the optical mode is maintained at 1533.9 nm. The intrinsic optical Q-factor and mechanical Q-factor in an ambient environment are 8.5×10^3 and 2.0×10^3, respectively, which are indicated by the optical transmission spectrum and the mechanical spectrum as shown in Fig. 3c and d.

In addition, owing to the design flexibility offered by the separate confinement of the optical and mechanical modes in the hetero structure, we were able to demonstrate a strong optomechanical coupling. The measured optomechanical coupling rate ($g_0/2\pi$) of the cavity was 1.9 MHz, which is the highest amongst reported optomechanical systems (Supplementary S5).

3.3. Phonon lasing and stimulated scattered photon

We demonstrate phonon lasing using the fabricated OMC cavity in silicon in the normal regime with $\Gamma \ll \kappa$. As mentioned above, for an optomechanical cavity with $\Gamma \ll \kappa$, low-noise mechanical motion can

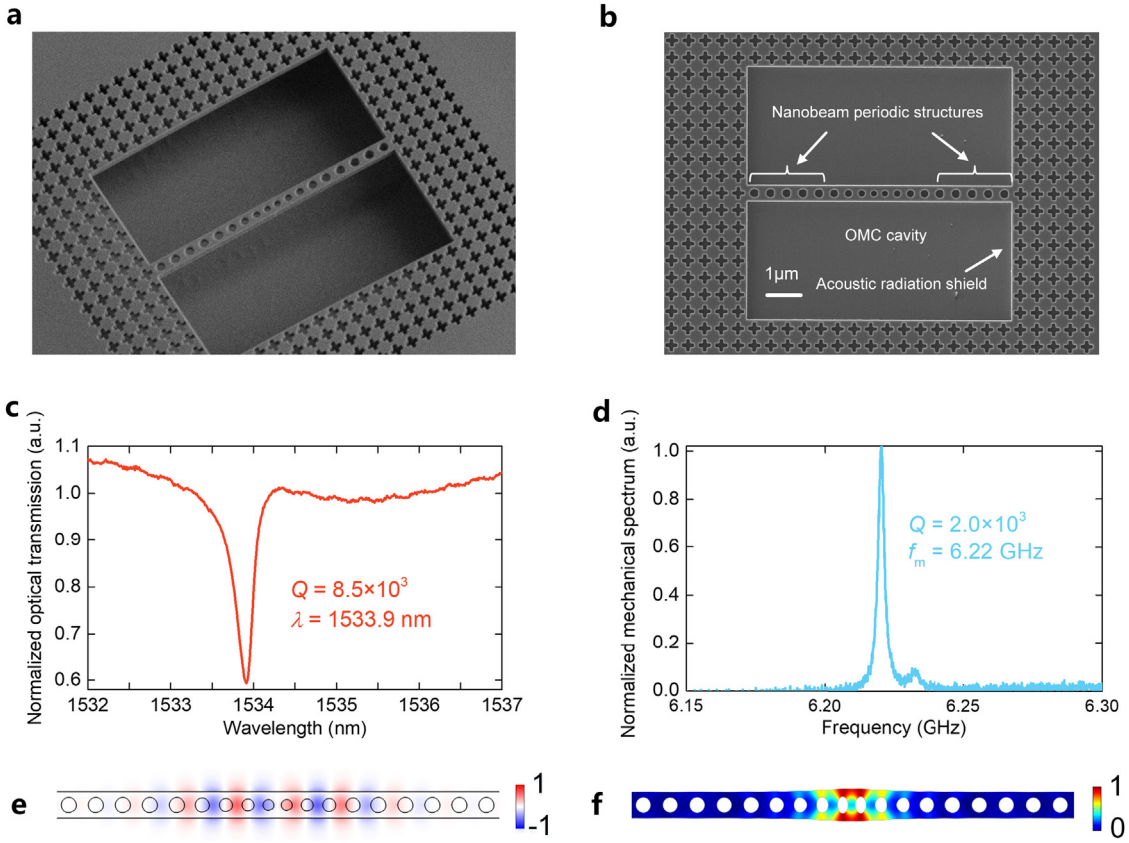

Fig. 3. (a) Oblique view and (b) top view of the scanning electron microscope (SEM) image of the OMC cavity with an acoustic radiation shield. (c) Optical and (d) mechanical spectra of the OMC cavity. (e) Transverse electric component of the cavity optical mode. (f) Displacement of the cavity mechanical mode.

be excited by a high-noise pump light. Thus, this regime has considerable potential for low-phase-noise applications. When we blue-detune the pump light with a linewidth of 2.0×10^2 kHz and increase its power, pronounced thresholds for both photons and phonons can be observed. Fig. 4a shows the normalised number of phonons in the cavity as a function of the coupled optical power. Here, the number of phonons is normalised to the number of phonons excited by the thermal environment, which is 1.01×10^3 at room temperature. Owing to the effective confinement of the optical and mechanical modes and the strong interaction between them in the OMC cavity, the threshold of the reduced optical power is 503 μW. Beyond this threshold, the number of phonons in the mechanical mode increases sharply, as shown in Fig. 4a, and the mechanical linewidth can be suppressed from 3.2 to 5.2 kHz, as shown in Fig. 4b, corresponding to an effective mechanical Q-factor of up to 1.2×10^6. We further analyse the suppressed mechanical linewidth and find that it follows the ST limit form as shown in Fig. 4b (Supplementary S6). The spectra of the spontaneous and stimulated phonon and scattering photon are shown in Fig. 4b. These experimental results are in good agreement with the aforementioned conclusion that the mechanical-lasing linewidth is much narrower than the linewidth of the pump laser.

Because the mechanical motion is characterised by the optical beat note between the scattering light and the pump light, the power of the scattering light can also be inferred (Supplementary S7). Fig. 4a shows the power of the scattering light versus the coupled optical power. Similar to the phonon number, the power of the scattering light increases sharply when the reduced pump power is beyond the threshold. In addition, because the linewidth of the beat signal changes from 3.2 MHz to 5.2 kHz and the linewidth of the pump laser itself is 2.0×10^2 kHz, it can be inferred that the linewidth of the scattering light is suppressed from around 3.2 MHz to 2.0×10^2 kHz, which is consistent with our theoretical prediction.

In addition, we measured the phonon linewidth excited by a pump laser with a linewidth of up to 50 MHz. The measured spectrum of the pump photon is shown in Fig. 3d. Although the linewidth of the pump is much greater than the intrinsic linewidth of the mechanical motion of 3.2 MHz, the linewidth of the excited phonon decreases to 5.4 kHz, which is four orders of magnitude narrower than the linewidth of the pump light. This is in good agreement with the simulation prediction shown in Fig. 2b, i.e. the ultra-low-noise mechanical signal can be excited even with a high-noise pump light, whereas the linewidths of the scattering photon and the pump light are similar.

4. Discussion and conclusion

Our theoretical analysis explained the dynamics underlying the lasing behaviour of a cavity optomechanical system. For systems in the normal regime with $\Gamma \ll \kappa$, a high-noise pump laser can excite an ultra-low-noise mechanical oscillation, and the low-noise signal can be directly detected by a photon detector from the high-noise pump laser without introducing additional noise. Moreover, the behaviour of the cavity optomechanical system is distinctly different from that of the Brillouin system in the reversed regime with $\Gamma \gg \kappa$, because the jitter in the equilibrium position is considerable and it influences the system significantly. The linewidth of the scattering photon is broader than the linewidth of the pump laser. However, the phonon linewidth is consistent with that of stimulated Brillouin scattering and it follows Eq. 9.

For experimental verification, we used a silicon-based OMC cavity with an acoustic radiation shield. We demonstrated both silicon-based photon and phonon lasers with phonon lasing at 6.22 GHz and scattering photon lasing at a wavelength of 1533.9 nm. The measured narrow linewidths for photon and phonon lasing were consistent with our theoretical predictions.

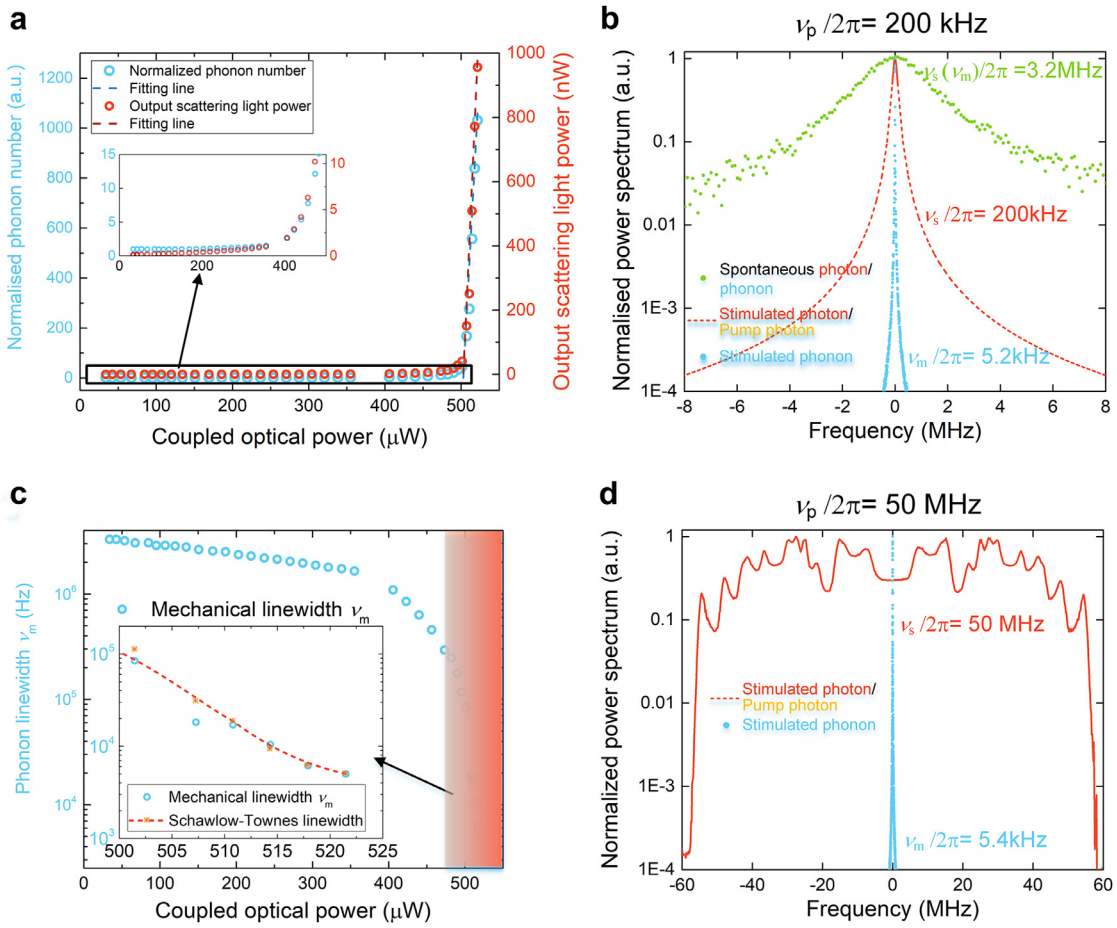

Fig. 4. Experimental demonstration of phonon lasing in the silicon-based OMC cavity. (a) Normalised number of phonons (blue) and output scattering light power (red) as a function of the coupled optical power (Supplementary S8). The inset shows the data below the threshold. It can be seen that lasing phonon and stimulated photon have an identical threshold (Supplementary S1). (b) Normalised power spectra of the spontaneous photon and phonon (green), stimulated photon (red), and stimulated phonon (blue) with a pump linewidth of 200 kHz (Supplementary S9). (c) Phonon linewidth as a function of the coupled optical power; the lasing zone is marked as a red gradient zone. The inset shows the calculated ST limit as a function of the coupled optical power. (d) Normalised power spectra of the stimulated photon (red) and the stimulated phonon (blue) with a pump linewidth of 50 MHz.

Our findings can pave the way towards photon and phonon lasers based on silicon, and they could enable researchers to meet the pressing need for new laser technologies for silicon-based photonic devices. Harnessing the coherence of photons and phonons in silicon devices could facilitate new applications in sensing, metrology, spectroscopy, and signal processing, thereby advancing the use of highly coherent sources.

Notably, our optomechanical-cavity-based scheme offers a footprint of only 120 μm^2, i.e. around three orders of magnitude smaller than that required by the Brillouin system [10], which requires a long optical path of several centimetres. Moreover, an experimental measurement [33] of the second-order correlation of scattering photon in OMC cavity (above phonon lasing threshold, $g^2(0) \sim 1$) suggests that the coherence of the stimulated photon is similar to a true photon laser, which can be a superior substitute for stimulated Brillouin scattering. Owing to the strong photon-phonon interaction in the OMC cavity, the threshold pump power required to achieve lasing is only 503 μW, which is lower than that of the Brillouin system (7.5 mW) by an order of magnitude [10]. Furthermore, our OMC system is compatible with silicon integrated devices, and it may provide an elegant approach for complementing stimulated Brillouin scattering, which is not only the strongest and most tuneable nonlinear interaction with considerable potential for high-coherence and ultra-low-noise oscillation but also particularly challenging to achieve on a silicon platform.

Declaration of competing interest

The authors declare that they have no conflicts of interest in this work.

CRediT authorship contribution statement

Jian Xiong: Conceptualization, Formal analysis, Methodology, Writing – original draft. **Zhilei Huang:** Conceptualization, Methodology, Writing – original draft. **Kaiyu Cui:** Conceptualization, Formal analysis, Writing – original draft. **Xue Feng:** Writing – review & editing. **Fang Liu:** Writing – review & editing. **Wei Zhang:** Writing – review & editing. **Yidong Huang:** Formal analysis.

Code availability

The custom code used in this study is available from the corresponding author upon reasonable request.

Data availability

The supporting data for the plots in this paper and other findings of this study are available from the corresponding author upon reasonable request.

Acknowledgments

The authors would also like to thank Innovation centre of Advanced Optoelectronic Chip and Institute for Electronics and Information Technology in Tianjin, Tsinghua University for their help with device fabrication. This work was supported by the National Key R&D Program of China under Contracts No. 2018YFB2200402, the National Natural Science Foundation of China (61775115, 91750206, 61575102, and 61621064), the Opened Fund of the State Key Laboratory on Integrated Optoelectronics (IOSKL2016KF01), and Beijing Innovation centre for Future Chips, Tsinghua University.

Supplementary materials

Supplementary material associated with this article can be found, in the online version, at doi:10.1016/j.fmre.2022.10.008.

References

[1] A. Kobyakov, M. Sauer, D. Chowdhury, Stimulated Brillouin scattering in optical fibers, Adv. Opt. Photonics 2 (2010) 1–59.
[2] I.S. Grudinin, A.B. Matsko, L. Maleki, Brillouin Lasing with a CaF2 whispering gallery mode resonator, Phys. Rev. Lett. 102 (2009) 043902.
[3] S.P. Smith, F. Zarinetchi, S. Ezekiel, Narrow-linewidth stimulated Brillouin fiber laser and applications, Opt. Lett. 16 (1991) 393–395.
[4] S. Gundavarapu, G.M. Brodnik, M. Puckett, et al., Sub-hertz fundamental linewidth photonic integrated Brillouin laser, Nat. Photonics 13 (2019) 60–67.
[5] J. Subías, C. Heras, J. Pelayo, et al., All in fiber optical frequency metrology by selective Brillouin amplification of single peak in an optical comb, Opt. Express 17 (2009) 6753–6758.
[6] C. Galindez, F.J. Madruga, J.M. Lopez-Higuera, Brillouin frequency shift of standard optical fibers set in water vapor medium, Opt. Lett. 35 (2010) 28–30.
[7] T. Kurashima, T. Horiguchi, M. Tateda, Distributed-temperature sensing using stimulated Brillouin scattering in optical silica fibers, Opt. Lett. 15 (1990) 1038–1040.
[8] X. Xue, X. Zheng, H. Zhang, et al., Widely tunable single-bandpass microwave photonic filter employing a non-sliced broadband optical source, Opt. Express 19 (2011) 18423–18429.
[9] S. Chin, L. Thévenaz, J. Sancho, et al., Broadband true time delay for microwave signal processing, using slow light based on stimulated Brillouin scattering in optical fibers, Opt. Express 18 (2010) 22599–22613.
[10] N.T. Otterstrom, R.O. Behunin, E.A. Kittlaus, et al., A silicon Brillouin laser, Science 360 (2018) 1113–1116.
[11] E.A. Kittlaus, N.T. Otterstrom, P. Kharel, et al., Non-reciprocal interband Brillouin modulation, Nat. Photonics 12 (2018) 613–619.
[12] R. Van Laer, B. Kuyken, D. Van Thourhout, et al., Interaction between light and highly confined hypersound in a silicon photonic nanowire, Nat. Photonics 9 (2015) 199–203.
[13] E.A. Kittlaus, H. Shin, P.T. Rakich, Large Brillouin amplification in silicon, Nat. Photonics 10 (2016) 463–467.
[14] T.J. Kippenberg, K.J. Vahala, Cavity optomechanics: back-action at the mesoscale, Science 321 (2008) 1172–1176.
[15] T.J. Kippenberg, K.J. Vahala, Cavity opto-mechanics, Opt. Express 15 (2007) 17172–17205.
[16] R. Riedinger, A. Wallucks, I. Marinković, et al., Remote quantum entanglement between two micromechanical oscillators, Nature 556 (2018) 473–477.
[17] E. Verhagen, S. Deléglise, S. Weis, et al., Quantum-coherent coupling of a mechanical oscillator to an optical cavity mode, Nature 482 (2012) 63–67.
[18] C. Dong, V. Fiore, M.C. Kuzyk, et al., Optomechanical dark mode, Science 338 (2012) 1609–1613.
[19] A.H. Safavi-Naeini, S. Gröblacher, J.T. Hill, et al., Squeezed light from a silicon micromechanical resonator, Nature 500 (2013) 185–189.
[20] J. Zhang, B. Peng, Ş.K. Özdemir, et al., A phonon laser operating at an exceptional point, Nat. Photonics 12 (2018) 479–484.
[21] I.S. Grudinin, H. Lee, O. Painter, et al., Phonon laser action in a tunable two-level system, Phys. Rev. Lett. 104 (2010) 2–5.
[22] T. Carmon, H. Rokhsari, L. Yang, et al., Temporal behavior of radiation-pressure-induced vibrations of an optical microcavity phonon mode, Phys. Rev. Lett. 94 (2005) 223902.
[23] H. Jing, S.K. Özdemir, X.Y. Lü, et al., PT-symmetric phonon laser, Phys. Rev. Lett. 113 (2014) 053604.
[24] W. Yu, W.C. Jiang, Q. Lin, et al., Cavity optomechanical spring sensing of single molecules, Nat. Commun. 7 (2016) 12311.
[25] K. Cui, Z. Huang, N. Wu, et al., Phonon lasing in a hetero optomechanical crystal cavity, Photonics Res. 9 (2021) 937–943.
[26] K.J. Vahala, Back-action limit of linewidth in an optomechanical oscillator, Phys. Rev. A 78 (2008) 023832.
[27] N. Lörch, J. Qian, A. Clerk, et al., Laser theory for optomechanics: limit cycles in the quantum regime, Phys. Rev. X 4 (2014) 011015.
[28] K.Y. Fong, M. Poot, X. Han, et al., Phase noise of self-sustained optomechanical oscillators, Phys. Rev. A 90 (2014) 023825.
[29] F. Marquardt, J.G.E. Harris, S.M. Girvin, Dynamical multistability induced by radiation pressure in high-finesse micromechanical optical cavities, Phys. Rev. Lett. 96 (2006) 103901.
[30] D.A. Rodrigues, A.D. Armour, Amplitude noise suppression in cavity-driven oscillations of a mechanical resonator, Phys. Rev. Lett. 104 (2010) 053601.
[31] M. Hossein-Zadeh, H. Rokhsari, A. Hajimiri, et al., Characterization of a radiation–pressure-driven micromechanical oscillator, Phys. Rev. A 74 (2006) 023813.
[32] H. Rokhsari, M. Hossein-Zadeh, A. Hajimiri, et al., Brownian noise in radiation-pressure-driven micromechanical oscillators, Appl. Phys. Lett. 89 (2006) 261109.
[33] J.D. Cohen, S.M. Meenehan, G.S. MacCabe, et al., Phonon counting and intensity interferometry of a nanomechanical resonator, Nature 520 (2015) 522–525.
[34] A. Debut, S. Randoux, J. Zemmouri, Experimental and theoretical study of linewidth narrowing in Brillouin fiber ring lasers, J. Opt. Soc. Am. B 18 (2001) 556–567.
[35] J. Li, H. Lee, T. Chen, et al., Characterization of a high coherence, Brillouin microcavity laser on silicon, Opt. Express 20 (2012) 20170–20180.
[36] A. Nunnenkamp, V. Sudhir, A.K. Feofanov, et al., Quantum-limited amplification and parametric instability in the reversed dissipation regime of cavity optomechanics, Phys. Rev. Lett. 113 (2014) 023604.
[37] M. Aspelmeyer, T.J. Kippenberg, F. Marquardt, Cavity optomechanics, Rev. Mod. Phys. 86 (2014) 1391–1452.
[38] P. Gallion, G. Debarge, Quantum phase noise and field correlation in single frequency semiconductor laser systems, IEEE J. Quantum Electron. 20 (1984) 343–349.
[39] V. Giovannetti, D. Vitali, Phase-noise measurement in a cavity with a movable mirror undergoing quantum Brownian motion, Phys. Rev. A 63 (2001) 023812.
[40] S. Sabhapandit, Work fluctuations for a harmonic oscillator driven by an external random force, EPL Europhys. Lett. 96 (2011) 20005.
[41] A. Debut, S. Randoux, J. Zemmouri, Linewidth narrowing in Brillouin lasers: theoretical analysis, Phys. Rev. A 62 (2000) 023803.
[42] L. Mandel, E. Wolf, Optical Coherence and Quantum Optics, Cambridge University Press, Cambridge, 1995.
[43] K. Yoshimura, K. Arai, Phase reduction of stochastic limit cycle oscillators, Phys. Rev. Lett. 101 (2008) 154101.
[44] A.G. Krause, J.T. Hill, M. Ludwig, et al., Nonlinear radiation pressure dynamics in an optomechanical crystal, Phys. Rev. Lett. 115 (2015) 233601.
[45] J.T. Hill, A.H. Safavi-Naeini, J. Chan, et al., Coherent optical wavelength conversion via cavity optomechanics, Nat. Commun. 3 (2012) 1196.
[46] D. Navarro-Urrios, N.E. Capuj, J. Gomis-Bresco, et al., A self-stabilized coherent phonon source driven by optical forces, Sci. Rep. 5 (2015) 15733.
[47] L.D. Tóth, N.R. Bernier, A. Nunnenkamp, et al., A dissipative quantum reservoir for microwave light using a mechanical oscillator, Nat. Phys. 13 (2017) 787–793.
[48] M. Eichenfield, J. Chan, R.M. Camacho, et al., Optomechanical crystals, Nature 462 (2009) 78–82.
[49] Z. Huang, K. Cui, Y. Li, et al., Strong optomechanical coupling in nanobeam cavities based on hetero optomechanical crystals, Sci. Rep. 5 (2015) 15964.
[50] Q. Xu, K. Cui, N. Wu, et al., Tunable mechanical-mode coupling based on nanobeam–double optomechanical cavities, Photonics Res. 10 (2022) 1819–1827.
[51] N. Wu, K. Cui, X. Feng, et al., Hetero-optomechanical crystal zipper cavity for multimode optomechanics, Photonics 9 (2022) 78.
[52] H. Lü, S.K. Özdemir, L.M. Kuang, et al., Exceptional points in random-defect phonon lasers, Phys. Rev. Appl. 8 (2017) 044020.

Jian Xiong received his Ph.D. degree (2022.06) in the Department of Electronic Engineering of Tsinghua University. His research interests focus on metasurface, nonlinear optics, and optomechanical crystals.

Zhilei Huang received his Ph.D. degree (2018.06) in the Department of Electronic Engineering of Tsinghua University. His research interests focus on nonlinear optics, photonic crystals and optomechanical crystals.

Kaiyu Cui is a tenured associate professor at the Department of Electronic Engineering in Tsinghua University, Beijing, China. Prof. Cui's research interests focus on metasurface, photonic crystals, and optomechanical crystals.